



HAL
open science

Impact of the Turbulent Vertical Mixing on Chemical and Cloud Species in the Venus Cloud Layer

Maxence Lefevre, Franck Lefèvre, Emmanuel Marcq, Anni Määttänen,
Aurélien Stolzenbach, Nicolas Streel

► To cite this version:

Maxence Lefevre, Franck Lefèvre, Emmanuel Marcq, Anni Määttänen, Aurélien Stolzenbach, et al..
Impact of the Turbulent Vertical Mixing on Chemical and Cloud Species in the Venus Cloud Layer.
Geophysical Research Letters, 2024, 51 (12), pp.e2024GL108771. 10.1029/2024gl108771. insu-04617342

HAL Id: insu-04617342

<https://insu.hal.science/insu-04617342v1>

Submitted on 19 Jun 2024

HAL is a multi-disciplinary open access archive for the deposit and dissemination of scientific research documents, whether they are published or not. The documents may come from teaching and research institutions in France or abroad, or from public or private research centers.

L'archive ouverte pluridisciplinaire **HAL**, est destinée au dépôt et à la diffusion de documents scientifiques de niveau recherche, publiés ou non, émanant des établissements d'enseignement et de recherche français ou étrangers, des laboratoires publics ou privés.



Distributed under a Creative Commons Attribution 4.0 International License

Geophysical Research Letters[®]

RESEARCH LETTER

10.1029/2024GL108771

Impact of the Turbulent Vertical Mixing on Chemical and Cloud Species in the Venus Cloud Layer



Key Points:

- Estimation for the first time of the spatial and temporal variability of chemical species due to vertical mixing
- Quantification of the vertical eddy diffusion coefficient, order of magnitude above typical used values
- Cloud-top altitudes change by 0.2–1 km due to vertical convective mixing and gravity waves

Supporting Information:

Supporting Information may be found in the online version of this article.

Correspondence to:

M. Lefèvre,
maxence.lefevre@latmos.ipsl.fr

Citation:

Lefèvre, M., Lefèvre, F., Marcq, E., Määttänen, A., Stolzenbach, A., & Streef, N. (2024). Impact of the turbulent vertical mixing on chemical and cloud species in the Venus cloud layer. *Geophysical Research Letters*, 51, e2024GL108771. <https://doi.org/10.1029/2024GL108771>

Received 9 FEB 2024

Accepted 3 JUN 2024

Maxence Lefèvre¹ , Franck Lefèvre¹ , Emmanuel Marcq¹ , Anni Määttänen¹, Aurélien Stolzenbach² , and Nicolas Streef¹ 

¹LATMOS/IPSL, Sorbonne Université, UVSQ Université Paris-Saclay, CNRS, Paris, France, ²Instituto de Astrofísica de Andalucía (IAA/CSIC), Granada, Spain

Abstract The Venusian atmosphere hosts a 10 km deep convective layer that has been studied by various spacecrafts. However, the impact of the strong vertical mixing on the chemistry of this region is still unknown. This study presents the first realistic coupling between resolved small-scale turbulence and a chemical network. The resulting vertical mixing is different for each species: those with longer chemical timescales will tend to be well-mixed. Vertical eddy diffusion due to resolved convection motions was estimated, ranging from 10^2 to 10^4 m²/s for the 48–55 km convective layer, several orders of magnitude above the typically used value. In the 48–55 km convective layer, the impact of the small-scale turbulence on the cloud layer boundaries was between 200 m and 1 km. The impact of turbulence on cloud chemistry is consistent with Venus Express/Visible and Infrared Thermal Imaging Spectrometer observations. The observability at the cloud-top of small-scale turbulence by VenSpec-U spectrometer would be challenging.

Plain Language Summary Venus hosts a global sulfuric acid cloud layer between 45 and 70 km. A convective layer is present between roughly 50 and 60 km, with its variability in latitude and local time assessed by observation, with a thicker layer at high latitude and at night. One question that remains unclear is how this turbulence mixes momentum, heat, and chemical species. Especially, the impact of the strong vertical mixing on the chemistry of this region is still unknown. To investigate this topic, we use a convection-resolving model coupled for the first time with a realistic chemical network. The resulting vertical mixing is different for each species: those with longer chemical timescales will tend to be well-mixed. 1D and global circulation models use the so-called vertical eddy diffusion approach to represent turbulent motion, quantified in our model and underestimated in chemistry models. The small-scale turbulence in the cloud layer causes a variation in the altitude of the top and bottom boundaries of the cloud. Our model shows that the impact of turbulence on cloud chemistry corresponds well to what has been observed by satellites. In the future, the EnVision mission will be able to observe chemical species at the small turbulence scales.

1. Introduction

The Venusian cloud layer hosts a convective activity that has been assessed since the beginning of Venus spacecraft exploration (Belton et al., 1976; Rossow et al., 1980). Various Radio occultation experiments studied convective activity (Hinson & Jenkins, 1995; Seiff et al., 1980), measuring a convective layer between 50 and 55 km of altitude. *Venus Express* and *Akatsuki* observed this turbulent layer, measuring a strong latitudinal (Tellmann et al., 2009) and local time variability (Imamura et al., 2017) of the depth of the layer. In addition to the convection layer in the deep cloud layer, the venus monitoring camera observed at 365 nm cellular features at the top of the cloud at about 70 km of altitude above the subsolar point, suggesting convective activity (Markiewicz et al., 2007; Titov et al., 2012). A convective layer at this altitude is the main hypothesis for these observed structures.

Regarding Venus cloud chemistry, several 1D models have been developed. The models of Yung et al. (2009), Krasnopolsky (2012), Bierson and Zhang (2020), and Rimmer et al. (2021) used a vertical eddy diffusion value that underrepresents the turbulent activity in the cloud layer (M. Lefèvre et al., 2022), and were not able to reproduce the observed vertical gradient of SO₂ in the clouds. The interaction between the turbulence and chemistry has been little studied, and is therefore poorly known. Only McGouldrick and Toon (2008) gave an insight into the change of optical depth due to the convection and gravity waves, using an idealized 2D (zonal/vertical) representation of the Venus cloud convective layer.

© 2024. The Author(s).

This is an open access article under the terms of the [Creative Commons Attribution License](https://creativecommons.org/licenses/by/4.0/), which permits use, distribution and reproduction in any medium, provided the original work is properly cited.

In order to investigate the turbulent activity inside the Venus cloud layer, we use the limited-area Venus mesoscale model (VMM) large-eddy simulation (LES) mode (M. Lefèvre et al., 2022) adapted from a terrestrial hydrodynamical solver (Skamarock & Klemp, 2008) to simulate only a specified region of the planet at a fine resolution. A complete photochemical scheme (Stolzenbach et al., 2023; Streeel et al., 2023) was coupled to the VMM. For the first time in Venusian atmospheric studies, a chemical network is coupled to a 3D convection resolving model, allowing the study of small-scale spatio-temporal variations. We will focus on the main active chemical species present in the cloud: SO₂, SO, H₂O and H₂SO₄ (the latter two in both liquid and gaseous forms).

2. Modeling

2.1. IPSL Venus LES Model

Our mesoscale model for Venus is based on the dynamical core of the Advanced Research Weather-Weather Research and Forecast (hereinafter referred to as weather research and forecast) terrestrial model (Skamarock & Klemp, 2008). Alongside solar and infrared heating rates calculated by the Institut Pierre-Simon Laplace (IPSL) Venus planetary climate model (PCM) radiative transfer (Lebonnois et al., 2015) using the cloud model is based on Haus et al. (2014, 2015), a third additional rate representing the heat from the large-scale circulation is imposed. The details of this last rate are described in detail in M. Lefèvre et al. (2017).

2.2. IPSL Photochemistry Model

The LES model is coupled to a photochemistry model described in detail in Stolzenbach et al. (2023). This photochemical model represents the comprehensive chemistries of CO₂ cycle, the sulfur oxidation cycle, and the chlorine cycle for neutral species from 35 to 100 km, meaning from $6 \cdot 10^5$ Pa–1 Pa and from 460 to 160 K. In addition, a nitrogen photochemical network has been included into the chemistry model (Streeel et al., 2023), with the addition of the four nitrogenous species N, N(^{2D}), NO, and NO₂. Our chemical network takes into account the 38 species in gas-phase and two liquid-phase species H₂SO₄ and H₂O, interacting through 123 chemical reactions.

In Stolzenbach et al. (2023), the photolysis calculation was performed off-line with a lookup table that was a function of the CO₂ column, SO₂ column, and solar zenith angle. Currently, following the same strategy as in the Mars version of the PCM (F. Lefèvre, Trokhimovskiy, et al., 2021), photolysis rates for CO₂, SO₂, H₂ and nitrogen species are calculated on-line.

The vertical profile of sulfur species, especially SO₂, is an issue that is ubiquitous in Venus chemistry modeling (Bierson & Zhang, 2020; Rimmer et al., 2021; Stolzenbach et al., 2023). The goal of this study is not to reproduce quantitative SO₂ cloud-top abundances, the question of vertical gradient of SO₂ into the clouds being beyond the scope of this paper, but to quantify variabilities due to the interaction between small-scale turbulence and chemical species.

2.3. Microphysics Model

The representation of clouds in the model is based on the hypothesis that clouds are at all times in a state of thermodynamic equilibrium: the condensation/evaporation of H₂SO₄ and H₂O follows the saturation vapor pressure profile over the calculated equilibrium H₂SO₄ aqueous solution. Clouds in the model are supposed to be at all times in a thermodynamic equilibrium: the condensation/evaporation of H₂SO₄ and H₂O follow the saturation vapor pressure profile over the calculated equilibrium H₂SO₄ aqueous solution. The partitioning of H₂SO₄ and H₂O between the gas and liquid phases is calculated at each call to the chemistry subroutine. The cloud particle size distributions for the three modes implemented are prescribed and are the same as in Table 5 from Stolzenbach et al. (2023). A sedimentation flux is also taken into account, based on the Stokes velocity for each particle mode, described in detail in Stolzenbach et al. (2023).

2.4. Simulation Settings

This study is focused on two latitudinal and two local time cases: the Equator and 75° at noon and midnight to capture variabilities due to convection activity variation (M. Lefèvre et al., 2018). The M. Lefèvre et al. (2018)'s equilibrium state at the Equator and 75° at noon and midnight are used as the initial state with the same resolution and time-step, that is, 400 m over the horizontal domain size of 60 km and 1 s. To ensure that the chemistry is represented adequately in the case of strong vertical wind speed, the photochemistry scheme is called every 10 s,

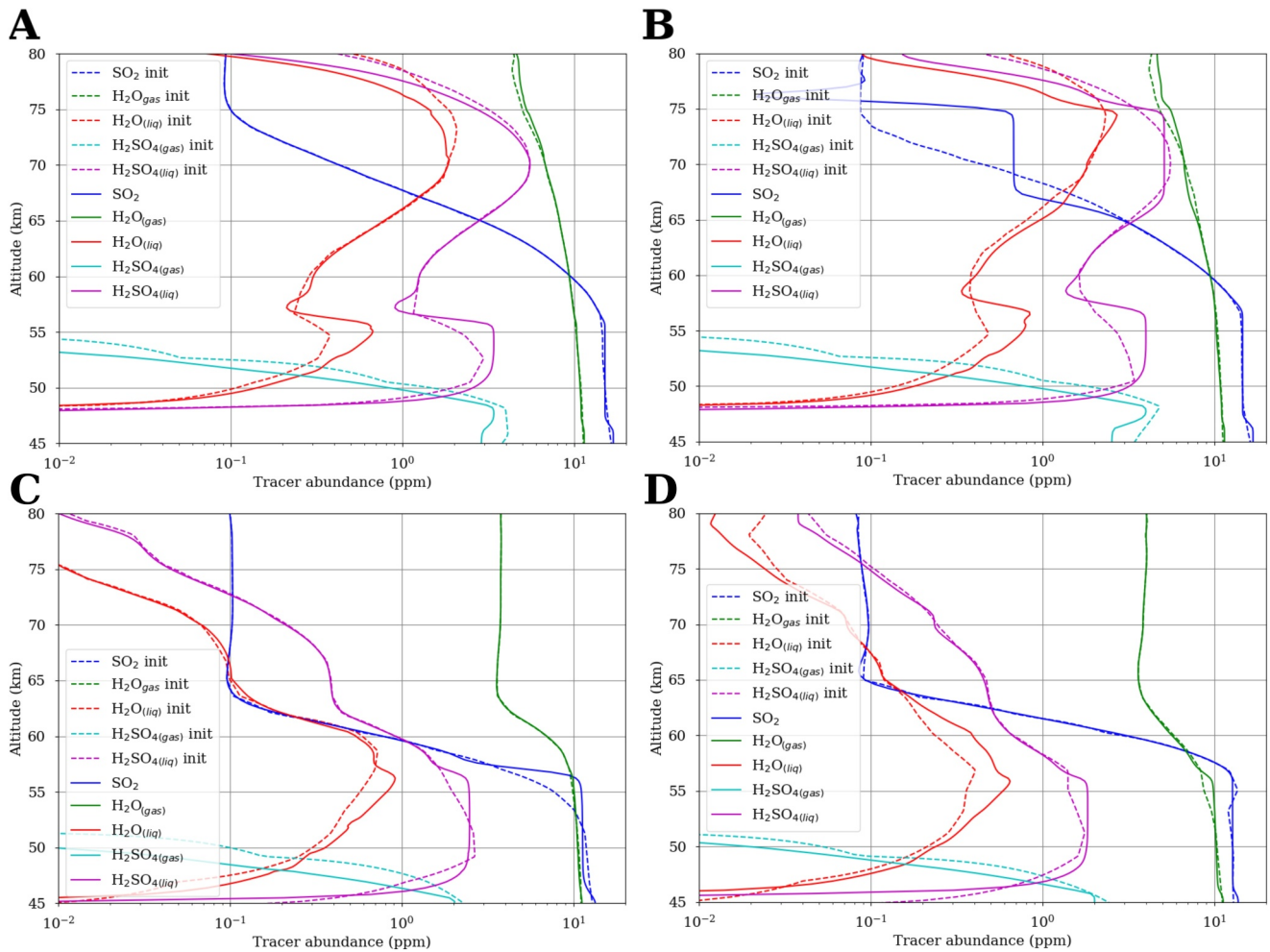


Figure 1. Domain averaged tracer abundance vertical profiles of SO₂ (blue lines), H₂O in the gas (green lines) and liquid phase (red lines), and H₂SO₄ in the gas (cyan lines) and liquid phase (magenta lines) at the Equator at midnight (a), noon (b), and at 75° of latitude at midnight (c) and noon (d). The solid lines represent the model outputs and the dotted lines the initial profile.

which is consistent with characteristic times of microphysical processes (James et al., 1997). Vertical profiles from Stolzenbach et al. (2023) are used as input for the chemistry scheme.

3. Vertical Mixing

3.1. Global Averaged Results

In the four panels of Figure 1, the convective layer is visible between roughly 48 and 55 km with the low vertical gradient meaning a strong vertical mixing, different for each species. For example, in this region, the vertical mixing ratio gradient of SO₂ is very low, whereas it is slightly larger for water. In M. Lefèvre et al. (2022), the vertical gradient due to mixing was dependent on the ratio between the chemical timescale and the convective layer dynamical timescale of $1.7 \cdot 10^4$ s. However, both SO₂ and H₂O vapor have long photochemical timescales, 10 Earth years below 55 km and 2 months above 55 km for SO₂, and about a decade for H₂O (all altitudes) (Stolzenbach, 2016). The difference between these two species is that water vapor can condense into droplets. The condensation timescale is around 10 s. The actual lifetime of water vapor is therefore much smaller than its photochemical timescale, leading to a weaker vertical mixing. Above the convective layer, both SO₂ and H₂O vapor decrease strongly.

The cloud top convective layer is also visible at the Equator at noon (Figure 1-B), with a strong vertical mixing between 67 and 75 km. Like for the 48–55 km convective layer, the effect of vertical mixing is different for each

species. SO₂ exhibits a weak vertical gradient, whereas for water this gradient is stronger due to condensation. At cloud-top altitudes, around 72 km, SO₂ mixing ratio at noon increases by a factor of four by convective mixing, going from 0.17 ppm at the initial state to 0.7 ppm. For the three other cases, gravity waves are present at cloud-top levels. Contrary to convective motions, these waves, emitted by the convection, generate a much smaller mixing for all species.

Another noticeable feature is the fact that the mixing ratio of condensed species tend to increase in the 48–55 km convective layer, conjugated with the decrease of the condensing vapor below the clouds. The convective motion will transport the condensable species, mainly H₂SO₄, from the below the clouds where the abundance is higher to the middle cloud region. The two vapors get depleted below 48 km, whereas the excess condenses in the lower and middle cloud, increasing the opacity of the clouds. This effect is weaker at high latitude due to lower temperatures affecting condensation. The large particles of the mode 3 represent the main source of cloud opacity. With mass coefficients for the different cloud droplet modes (Stolzenbach et al., 2023), the mass column density was calculated (Figure S1 in Supporting Information S1). The mass column at the Equator is 30% larger than the PCM column due to the resolved convection at both local times. If separated between updrafts and downdraft, the difference in the mass column is about 10%. At high latitude, the average increase due to convection is only of 15% compared to the PCM. This difference is due to the condensable reservoir that is much lower at high latitude because of the Hadley Cell circulation (Stolzenbach et al., 2023).

3.2. Effective Vertical Eddy Diffusion

In order to account for the subgrid scale turbulence, 1D models and 3D GCMs use a diffusion equation as a parametrization, with the vertical eddy diffusion coefficient (or K_{zz}) controlling the strength of the mixing processes.

In the Venusian atmosphere, the K_{zz} parameter has been estimated both from observations and modeling, but is still not well-constrained. The *Pioneer Venus* radio scintillation measurements estimated K_{zz} between 2 · 10⁻¹ m² s⁻¹ at 45 km (Woo et al., 1982) and 4 m² s⁻¹ at 60 km (Woo & Ishimaru, 1981). Using the values of the vertical wind measured in the deep cloud layer by the *VeGa* balloons (Sagdeev et al., 1986), K_{zz} was evaluated at 10³ m² s⁻¹ at 54 km (Blamont et al., 1986). K_{zz} was estimated with the vertical profile of H₂SO₄ vapor obtained by Venus Express (VEX)/VeRa radio-occultation between 10⁴ and 10⁵ m² s⁻¹ (Dai et al., 2023). Karyu et al. (2024) estimated K_{zz} around 2 m² s⁻¹ between 60 and 70 km with a 1D chemical model fitting Venus Express observations.

To quantify the vertical mixing of tracers, we define an effective eddy diffusion coefficient K_{z_{ef}} where the interaction of the resolved turbulence, like convection, and chemical processes are taken into account. This coefficient K_{z_{ef}} is calculated as follows:

$$K_{z_{ef}} = -\frac{\langle q'w' \rangle}{\partial \langle q \rangle / \partial z} \quad (1)$$

with q a tracer mixing ratio, primed quantities representing perturbations relative to the domain averaged values, and bracket quantities representing domain averaged values. The vertical wind field w' will be the same for each species, but chemical timescale is specific, leading to different q' .

As discussed in the previous section, the effect of vertical mixing is different for each species, and this is clearly seen in the K_{z_{ef}} values shown in Figure 2. For example, SO₂ and H₂O have different vertical gradients illustrating the difference in the mixing strength, and thus they have different K_{z_{ef}} values, around 10³ m² s⁻¹ for SO₂ and 10² m² s⁻¹ for H₂O. The values for the 48–55 km convective layer are quite constant between night and day. Above the convective layer, the turbulence is due mainly to small-scale gravity waves that engender a weak mixing, consistent with the Woo and Ishimaru (1981) measurements. The variability of the diurnal 48–55 km convective activity is visible, with K_{z_{ef}} stronger at night by a factor of two. At 75° degrees of latitude, the vertical mixing is stronger in the convective region by almost a factor 10, with K_{z_{ef}} reaching 10³ m² s⁻¹. Both below and above the convective layer, gravity waves are imposing a weaker vertical mixing, with values 10⁻¹ and 10 m² s⁻¹. The values inside the 48–55 km convective layer are consistent with in situ measurements (Blamont et al., 1986; Woo et al., 1982; Woo & Ishimaru, 1981). At the Equator at noon, the presence of the cloud-top convective layer

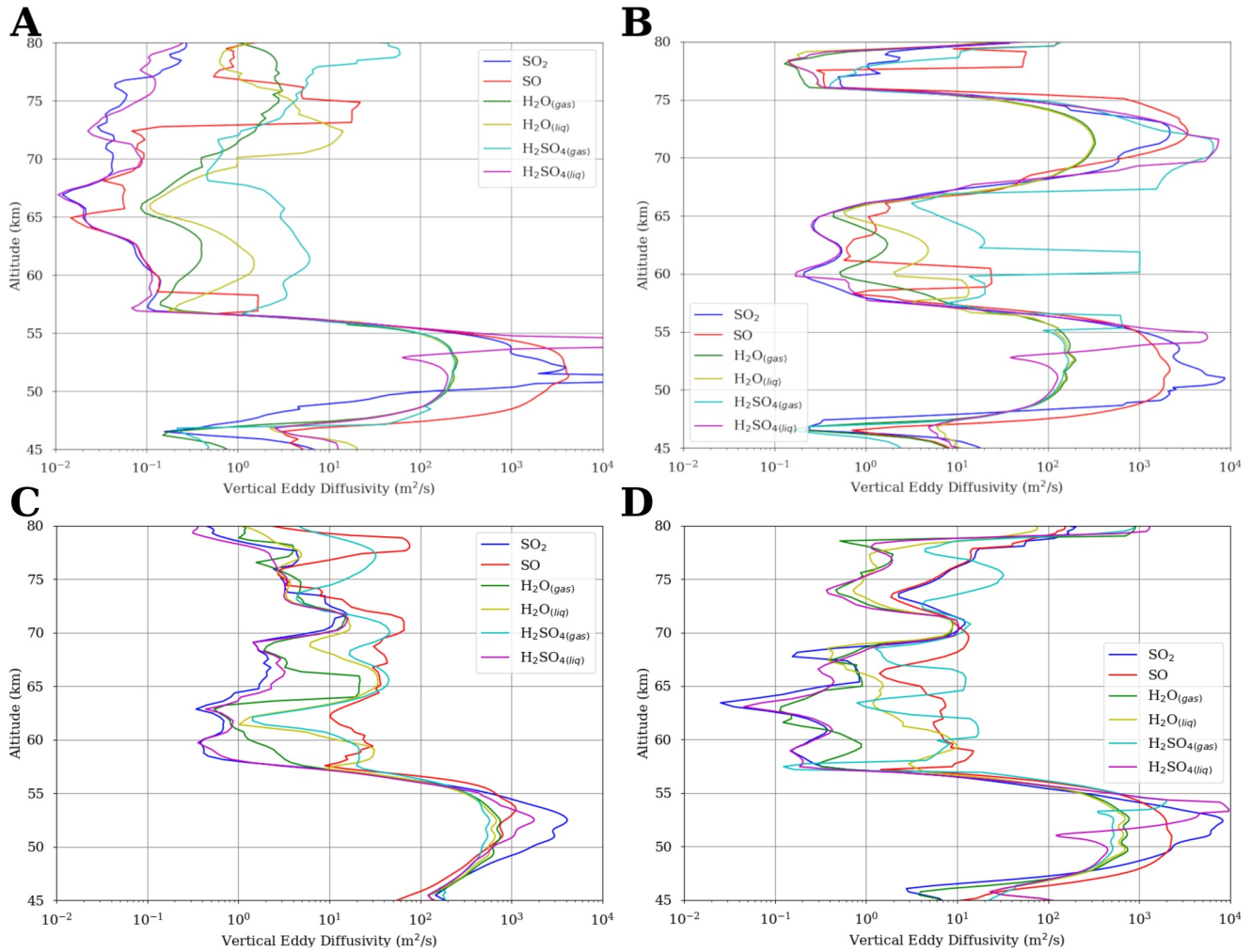


Figure 2. Vertical profiles of the vertical eddy diffusivity ($\text{m}^2 \text{s}^{-1}$) in the Venus cloud region calculated for SO_2 (blue lines), H_2O in the gas (green lines) and liquid phase (red lines), and H_2SO_4 in the gas (cyan lines) and liquid phase (magenta lines) at the Equator at midnight (left) and noon (right). For clarity, the vertical profiles are smoothed. Original profiles are available in Figure S2 in Supporting Information S1.

is visible with an increase of K_{zef} between 66 and 75 km, from $1 \text{ m}^2 \text{ s}^{-1}$ at 65 km to around $10^4 \text{ m}^2 \text{ s}^{-1}$ at 72 km. These cloud-top values of K_{zef} are slightly larger than the value for the 48–55 km convective layer. The H_2SO_4 vapor in the 48–55 km convective layer has a K_{zef} between 10^2 and $10^3 \text{ m}^2 \text{ s}^{-1}$, more than one order of magnitude lower than the highest estimation from radio-occultations (Dai et al., 2023). Outside the cloud-top convective layer at night, the values of K_{zef} are consistent with estimation from the modeling of Karyu et al. (2024). Inside the cloud-top convective layer, the value from the resolved convective layer is several order of magnitude higher.

Regarding the vertical mixing parametrization, the value of K_{zz} in the cloud region is often considered as a tunable parameter. The Krasnopolsky (2012) 1D model uses an eddy diffusion of $1 \text{ m}^2 \text{ s}^{-1}$ in the convective layer, whereas Bierson and Zhang (2020) defined several eddy diffusion scenarios for the convective layer mixing parametrization, from 0.1 to $2 \text{ m}^2 \text{ s}^{-1}$. Rimmer et al. (2021) also tested a range of vertical eddy diffusion values in the convective layer, between 0.01 and $1 \text{ m}^2 \text{ s}^{-1}$. These values are lower by several orders of magnitude compared to the turbulent vertical mixing we obtained with the coupled LES-chemistry model in this work, and thus are inconsistent with the present study and the in situ measurements by Blamont et al. (1986), Woo et al. (1982), and Woo and Ishimaru (1981).

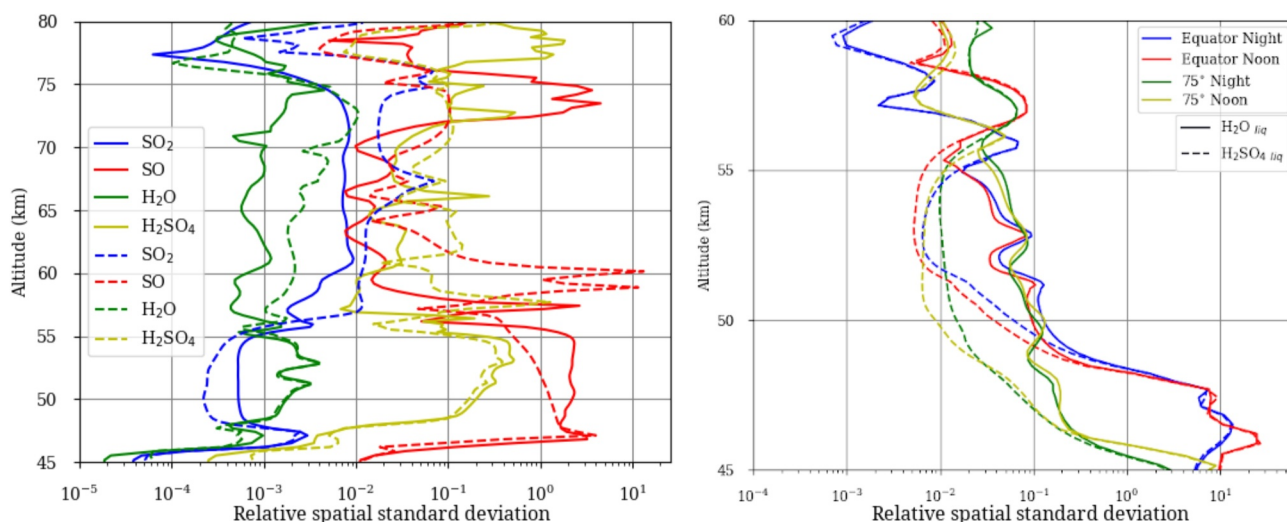


Figure 3. Left: Vertical profiles of the relative standard deviation for SO₂, SO, H₂O and H₂SO₄ in gas phase at the equator at night (solid line) and noon (dashed line). Right: Vertical profiles of the relative standard deviation for the condensed phase of H₂SO₄ and H₂O at the equator (solid line) and 75° (dashed line) for the studied local time.

4. Spatial and Temporal Variability

In the 48–55 km convective layer, the spatial standard deviation is larger at night, with more vivid convective motions. At higher altitudes, the standard deviation is again larger in the cloud-top convective layer and due to the trapped gravity waves that have a large amplitude.

SO₂ exhibits the lowest standard deviation in the 48–55 km convective layer due to a very strong vertical mixing seen in Figure 1. On the contrary, SO exhibits the highest spatial variabilities. At cloud-top altitudes, SO has a lifetime of about 30 min due to quick photolysis processes. This lifetime is of the same order of magnitude as the dynamical timescale of the cloud-top convection, leading to high spatial variability (M. Lefèvre, Trokhimovskiy, et al., 2021). In the 48–55 km convective layer, the lifetime of SO is much longer due to the lack of photons at these altitudes, but the vertical gradient is strong, going at the Equator from 10⁻¹⁰ ppm at 48 km to 10⁻⁴ ppm at 55 km at night and from 10⁻⁵ ppm at 48 km to 10⁻³ ppm at 55 km at noon. There will be SO-poor ascending plumes and SO-rich descending plumes, leading to a high spatial variability due to convective mixing.

The spatial variability for the condensed species is shown in Figure 3-right. The variability is higher at lower latitudes due to the Hadley circulation that generates a strong latitudinal gradient for the gas phase of H₂O and H₂SO₄. The variability is also stronger for condensed water above the 48–55 km convection layer because of higher mixing ratio of water at this altitude range. The higher variability of the condensed species inside the 48–55 km exhibits the strong non-linearity of the condensation processes.

The dynamical timescale of the deep and cloud-top convective layer can be calculated as $\tau_{dyn} = H/\sigma_w$, with H being the scale height and σ_w the spatial standard deviation of the vertical wind at a given altitude. M. Lefèvre et al. (2022) estimated this timescale to be 17,000 s at 50 km and 6,000 s at 70 km. Coupled with the zonal wind flow, using high-frequency over several hours, the temporal variability timescale of chemical species is approximately 20 min inside the 48–55 km convective layer with an Eulerian perspective.

5. Impact on Cloud Boundary Altitudes

Convective layers are present at the bottom of the cloud layer, both at night and day, and at cloud-top altitudes at the subsolar point only, and can therefore impact altitudes of the cloud boundaries. For the bottom altitude, it is pretty straightforward to define, since the abundance of condensed species drops drastically to zero below the H₂SO₄/H₂O saturation level. However, for the cloud top, it is more subtle as the condensed species abundance decreases more gradually with increasing height. In order to calculate the cloud top elevation Z_{top} , we resolve the following equation: $\int_{Z_{top}}^{\infty} x(z)\rho_{gas}(z) dz = M_0$ where M_0 is the condensed species mass column density yielding an optical depth equal to one at 250 nm, x the mass mixing ratio of condensed species, and ρ_{gas} the density of the gas.

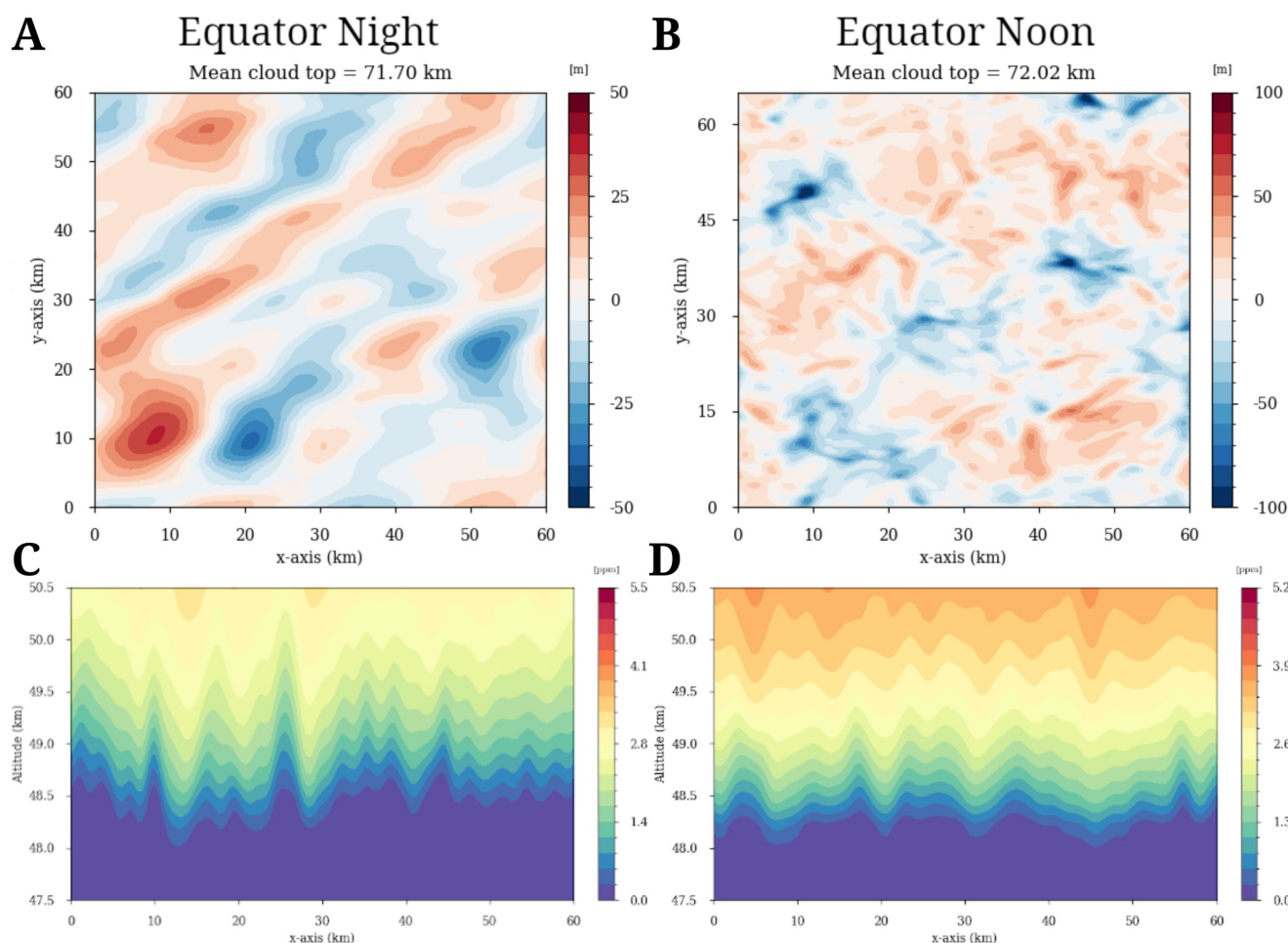


Figure 4. Top: Instantaneous cloud top altitude at the equator at midnight (left) and noon (right). Bottom: Instantaneous vertical cross-sections of gaseous H_2SO_4 at the equator at midnight (left) and noon (right).

For cloud top altitudes, using the radiative transfer model from Marcq et al. (2020), M_0 is equal to 0.29 μm at 250 nm.

There is only a limited diurnal variability of cloud-top and cloud-bottom altitudes, around 71 and 48 km respectively. At 75° (not shown), the cloud top is reaching altitudes of 61 km and the cloud bottom is around 45 km. These values are consistent with observations (Barstow et al., 2012; Ignatiev et al., 2009). However, at the cloud top there is a strong difference of horizontal structure of the cloud-top altitude. At the Equator at noon, the subsolar convective layer generates a displacement of the cloud of around 200 m, with ~ 20 km diameter convective updraft cells with narrow downdrafts. For the other cases, gravity waves at night induce a much smaller cloud-top variability visible in Figure 4-A, no larger than 100 m, with the 30 km horizontal wavelength waves visible (Peralta et al., 2008; Piccialli et al., 2014).

At the cloud bottom, the convective layer is present at all local times and latitudes but is slightly more intense at night and at high latitudes (M. Lefèvre et al., 2018), leading to a stronger vertical variability of the cloud bottom. At the Equator, the amplitude of the variations is around 600 m at night against 300 m at noon, with structures of 5 km wide. At 75° (not show), with a stronger convective layer, the amplitude of the variation of the cloud bottom reaches 600 m at noon against almost a 1 km at night, with horizontal structure over 10 km wide.

6. Discussion

VeGa 1 and *VeGa 2* measurements of SO_2 (Bertaux et al., 1996) and H_2O vapor (Surkov et al., 1986) in lower clouds are the only ones with a high vertical resolution. Inside the convective layer, SO_2 exhibits strong and

opposite vertical gradients and values that differ by a factor of three, incompatible with a well-mixed species. For H₂O vapor, a small vertical gradient between 50 and 60 km was observed, compatible with the presence of a convective layer, but the mixing ratio measured is several orders of magnitude higher than measurements obtained later from remote sensing orbiters (Marcq et al., 2023).

The large probe cloud particle size spectrometer experiment on Pioneer Venus (Knollenberg et al., 1980) and VENERA 9, 10, and 11 (Marov et al., 1980) measured cloud microphysical properties, such as extinction coefficient, scattering coefficient, backscattering, and number density with high vertical sampling. The probes showed that these properties are almost constant in the middle cloud region, approximately between 51 and 57 km. This corresponds to the region of the well-mixed liquid phase of H₂SO₄, suggesting that the middle cloud is strongly influenced by vertical mixing due to convection.

Ground telescopes have observed local time variations of SO₂ faster than few hours (Encrenaz et al., 2013, 2016), with an increase of a factor 5, indicating convective activity. The local injection of SO₂ by cloud-top convection is one of the main hypotheses for the long-term variations of SO₂ at cloud top (Marcq et al., 2013, 2020). The observed plumes are located near the Equator but are not increasingly present around noon (Encrenaz et al., 2019), therefore not consistent with the cloud-top convection presented here. In Figure 1, the vertical mixing at the subsolar point can increase the SO₂ mixing ratio by a factor 4. A study with a global model is necessary to test this hypothesis.

VEX/Visible and Infrared Thermal Imaging Spectrometer (VIRTIS) measured H₂O vapor inside the convective-like features at the subsolar point (Cottini et al., 2012), showing a variability inferior to 1 ppm and a variability of the cloud-top altitude around 500 m. Our model exhibits a variability of 0.3 ppm and a cloud-top variability around 200 m. The model underestimates these variabilities, but the result is consistent with convective cells at the lower edge of their estimated diameter (Markiewicz et al., 2007). The convection-induced cloud-top altitude variability is consistent with the Akatsuki measurement for the convective-like cells (Sato et al., 2020). Short-scale spatial and temporal (inferior to the 4 days atmospheric rotation rate) variability of SO₂ column density was observed with SPICAV (Vandaele et al., 2017), suggesting of turbulence activity. Radio occultation onboard Venus Express also observed gaseous H₂SO₄ (Oschlisniok et al., 2021), with variability larger than the one predicted by the model that cannot be accounted for turbulent processes. Oschlisniok et al. (2021) also reported radio occultation measurements of SO₂ but the spatial and temporal resolution is too coarse to be able to compare it with our model outputs. VIRTIS measured middle and lower cloud features, and a larger variability was observed at low latitudes (McGouldrick et al., 2008), an associated timescale of 30 hr corresponding to an eddy diffusion of 250 m² s⁻¹ (McGouldrick et al., 2012). These two observations are consistent with the resolved variability and vertical mixing of cloud droplets in the convective layer (Figure 3-right and Figure 2).

NASA's VERITAS and DAVINCI and ESA's EnVision are future space missions that will study cloud chemistry. The DAVINCI mission (Garvin et al., 2022) will use the mass spectrometer VMS and the laser Spectrometer Venus Tunable Laser Spectrometer (VTLS) to measure, H₂O, SO₂, OCS and CO from 64 km to the ground with high vertical sampling, and potentially record turbulent activity. The EnVision spacecraft will host a UV spectrometer VenSpec-U (Marcq et al., 2021) to measure SO₂, SO:SO₂ ratio, and the unknown UV absorber at cloud-top altitudes. An IR spectrometer VenSpec-H will measure H₂O, HDO, OCS, CO, and SO₂ between 65 and 80 km (Robert et al., 2019). Figures S3 and S4 in Supporting Information S1 show respectively SO₂ and the SO:SO₂ mixing ratio maps at cloud-top altitudes at the subsolar point. Convective cells are visible in SO₂ and SO with different structures due to chemical lifetime differences. The variability in SO₂ would be challenging to measure, and no convective structure is discernible for the SO:SO₂ ratio with a 12 km resolution. Figure S5 in Supporting Information S1 shows maps of CO, OCS, H₂O and HCl at cloud-top altitudes at the Equator at night and noon at the model resolution. The spatial resolution of VenSpec-H will be close to 100 km, limiting the turbulent activity's impact on observations. A radio-science experiment will also be present (Dumoulin et al., 2020), measuring convective layer depth and H₂SO₄ content in vapor and liquid from 35 to 55 km.

7. Conclusion

In this study, we present the first coupling between a resolved turbulence model and a chemical model for the Venus' atmosphere.

The impact of the strong vertical motion on different chemical species is estimated. The engendered vertical mixing is different for each species. Molecules with long chemical timescales will tend to be very well-mixed. For water, the condensation being a fast process, the vertical mixing inside the 48–55 km convective layer is weaker than for SO₂. This convective layer tends to increase the optical depth of the clouds, by bringing H₂SO₄ vapor-rich air from below the cloud, the vapor condensing into droplets during the ascent. The increase of opacity of the clouds due to this increase was quantified.

With the resolved convective motions, an estimation of the vertical eddy diffusion is possible. Values from 10² to 10⁴ m² s⁻¹ for the 48–55 km convective layer are calculated. This range of values is several orders of magnitude larger than the values generally used in 1D chemistry modeling. In order to represent with accuracy the convective mixing inside the cloud layer, realistic values of vertical eddy diffusion must be implemented.

With a simplified microphysics, for the first time, the impact of the small-scale turbulence on the cloud layer boundaries was estimated. At the bottom of the cloud layer, convective motions are ubiquitous, generating altitude variation of between 300 m and 1 km depending on the convective strength. At the cloud-top, the presence of gravity waves emitted by the 48–55 km convective layer generates only small variation of the cloud top altitude inferior to 100 m. At the subsolar point, the cloud-top convective layer generates displacements of the cloud top of the order of 200 m.

The convection-induced cloud-top altitude variability in the model is consistent with measurements by Venus Express and Akatsuki. The impact of turbulence on cloud chemistry is consistent with some past observations. In situ measurement of clouds properties in the lower and middle cloud shows constant profiles consistent with the strong mixing of H₂SO₄ liquid phase by the convection in this region.

The observability of the small-scale turbulence was assessed. EnVision with VenSpec-U would be able to resolve the spatial variability of SO₂ due to convection at cloud-top altitudes.

This first version of the coupled LES-chemistry-cloud model will be improved in the future. The equilibrium cloud parameterization used here will be replaced by a full microphysical model for the clouds that accounts for nucleation and growth of cloud droplets (Määttä et al., 2023).

Regarding the sulfur and water cycle, several species like S_n, H₂S can act as buffers of sulfur species and could be added into the chemical network. These two examples will also be measured by DAVINCI. The current formalism of the radiative transfer in the model does not account for cloud radiative feedback. This effect should be taken into account in future studies to provide a more realistic description of the Venusian cloud dynamics.

Data Availability Statement

The Simulation outputs used to obtain the results in this paper are available in the open online repository M. Lefèvre (2024).

References

- Barstow, J. K., Tsang, C. C. C., Wilson, C. F., Irwin, P. G. J., Taylor, F. W., McGouldrick, K., et al. (2012). Models of the global cloud structure on Venus derived from Venus Express observations. *Icarus*, 217(2), 542–560. <https://doi.org/10.1016/j.icarus.2011.05.018>
- Belton, M. J. S., Smith, G. R., Schubert, G., & del Genio, A. D. (1976). Cloud patterns, waves and convection in the Venus atmosphere. *Journal of the Atmospheric Sciences*, 33(8), 1394–1417. [https://doi.org/10.1175/1520-0469\(1976\)033<1394:CPWACI>2.0.CO;2](https://doi.org/10.1175/1520-0469(1976)033<1394:CPWACI>2.0.CO;2)
- Bertaux, J.-L., Widemann, T., Hauchecorne, A., Moroz, V. I., & Ekonomov, A. P. (1996). VEGA 1 and VEGA 2 entry probes: An investigation of local UV absorption (220–400 nm) in the atmosphere of Venus (SO₂, aerosols, cloud structure). *Journal of Geophysical Research*, 101(E5), 12709–12746. <https://doi.org/10.1029/96JE00466>
- Bierson, C. J., & Zhang, X. (2020). Chemical cycling in the Venusian atmosphere: A full photochemical model from the surface to 110 km. *Journal of Geophysical Research (Planets)*, 125(7), e06159. <https://doi.org/10.1029/2019JE006159>
- Blamont, J. E., Young, R. E., Seiff, A., Ragent, B., Sagdeev, R., Linkin, V. M., et al. (1986). Implications of the VEGA balloon results for Venus atmospheric dynamics. *Science*, 231(4744), 1422–1425. <https://doi.org/10.1126/science.231.4744.1422>
- Cottini, V., Ignatiev, N. I., Piccioni, G., Drossart, P., Grassi, D., & Markiewicz, W. J. (2012). Water vapor near the cloud tops of Venus from Venus Express/VIRTIS dayside data. *Icarus*, 217(2), 561–569. <https://doi.org/10.1016/j.icarus.2011.06.018>
- Dai, L., Shao, W., Gu, H., & Sheng, Z. (2023). Determination of the eddy diffusion in the Venusian clouds from VeRa sulfuric acid observations. *Astronomy and Astrophysics*, 679, A155. <https://doi.org/10.1051/0004-6361/202347714>
- Dumoulin, C., Rosenblatt, P., Tellmann, S., Genova, A., Marty, J.-C., Pätzold, M., et al. (2020). EnVision radio science experiment. In *European planetary science congress* (Vol. 13), EPSC2020–755. <https://doi.org/10.5194/epsc2020-755>
- Encrenaz, T., Greathouse, T. K., Marcq, E., Sagawa, H., Widemann, T., Bézard, B., et al. (2019). HDO and SO₂ thermal mapping on Venus. IV. Statistical analysis of the SO₂ plumes. *Astronomy and Astrophysics*, 623, A70. <https://doi.org/10.1051/0004-6361/201833511>

Acknowledgments

ML acknowledges support by a postdoctoral Grant from France's Centre National d'Études Spatiales (CNES). This project has received funding from the European Union's Horizon Europe research and innovation program under the Marie Skłodowska-Curie Grant agreement 101110489/MuSICA-V. ML would like to acknowledge the use of Sorbonne Université SACADO service unit. EM acknowledges support from CNES and ESA for all EnVision-related activities.

- Encrenaz, T., Greathouse, T. K., Richter, M. J., DeWitt, C., Widemann, T., Bézard, B., et al. (2016). HDO and SO₂ thermal mapping on Venus. III. Short-term and long-term variations between 2012 and 2016. *Astronomy and Astrophysics*, 595, A74. <https://doi.org/10.1051/0004-6361/201628999>
- Encrenaz, T., Greathouse, T. K., Richter, M. J., Lacy, J., Widemann, T., Bézard, B., et al. (2013). HDO and SO₂ thermal mapping on Venus. II. The SO₂ spatial distribution above and within the clouds. *Astronomy and Astrophysics*, 559, A65. <https://doi.org/10.1051/0004-6361/201322264>
- Garvin, J. B., Getty, S. A., Arney, G. N., Johnson, N. M., Kohler, E., Schwer, K. O., et al. (2022). Revealing the mysteries of Venus: The DAVINCI mission. *The Planetary Science Journal*, 3(5), 117. <https://doi.org/10.3847/PSJ/ac63e2>
- Haus, R., Kappel, D., & Arnold, G. (2014). Atmospheric thermal structure and cloud features in the southern hemisphere of Venus as retrieved from VIRTIS/VEX radiation measurements. *Icarus*, 232, 232–248. <https://doi.org/10.1016/j.icarus.2014.01.020>
- Haus, R., Kappel, D., & Arnold, G. (2015). Radiative heating and cooling in the middle and lower atmosphere of Venus and responses to atmospheric and spectroscopic parameter variations. *Planetary and Space Science*, 117, 262–294. <https://doi.org/10.1016/j.pss.2015.06.024>
- Hinson, D. P., & Jenkins, J. M. (1995). Magellan radio occultation measurements of atmospheric waves on Venus. *Icarus*, 114(2), 310–327. <https://doi.org/10.1006/icar.1995.1064>
- Ignatiev, N. I., Titov, D. V., Piccioni, G., Drossart, P., Markiewicz, W. J., Cottini, V., et al. (2009). Altimetry of the Venus cloud tops from the Venus express observations. *Journal of Geophysical Research (Planets)*, 114(E9). <https://doi.org/10.1029/2008JE003320>
- Imamura, T., Ando, H., Tellmann, S., Pätzold, M., Häusler, B., Yamazaki, A., et al. (2017). Initial performance of the radio occultation experiment in the Venus orbiter mission Akatsuki. *Earth Planets and Space*, 69(1), 137. <https://doi.org/10.1186/s40623-017-0722-3>
- James, E. P., Toon, O. B., & Schubert, G. (1997). A numerical microphysical model of the condensational Venus cloud. *Icarus*, 129(1), 147–171. <https://doi.org/10.1006/icar.1997.5763>
- Karyu, H., Kuroda, T., Imamura, T., Terada, N., Vandaele, A. C., Mahieux, A., & Viscardy, S. (2024). One-dimensional microphysics model of Venusian clouds from 40 to 100 km: Impact of the middle-atmosphere eddy transport and SOIR temperature profile on the cloud structure. *The Planetary Science Journal*, 5(3), 57. <https://doi.org/10.3847/PSJ/ad25f3>
- Knollenberg, R., Travis, L., Tomasko, M., Smith, P., Ragert, B., Esposito, L., et al. (1980). The clouds of Venus—A synthesis report. *Journal of Geophysical Research*, 85(A13), 8059–8081. <https://doi.org/10.1029/JA085iA13p08059>
- Krasnopolsky, V. A. (2012). A photochemical model for the Venus atmosphere at 47–112 km. *Icarus*, 218(1), 230–246. <https://doi.org/10.1016/j.icarus.2011.11.012>
- Lebonnois, S., Eymet, V., Lee, C., & Vatat d'Ollone, J. (2015). Analysis of the radiative budget of the Venusian atmosphere based on infrared Net Exchange Rate formalism. *Journal of Geophysical Research: Planets*, 120(6), 1186–1200. <https://doi.org/10.1002/2015JE004794>
- Lefèvre, F., Trokhimovskiy, A., Fedorova, A., Baggio, L., Lacombe, G., Määttäinen, A., et al. (2021). Relationship between the ozone and water vapor columns on Mars as observed by SPICAM and calculated by a global climate model. *Journal of Geophysical Research (Planets)*, 126(4), e06838. <https://doi.org/10.1029/2021JE006838>
- Lefèvre, M. (2024). Impact of the turbulent vertical mixing on chemical and cloud species in the Venus cloud layer [Dataset]. [figshare. https://doi.org/10.6084/m9.figshare.24972801.v1](https://doi.org/10.6084/m9.figshare.24972801.v1)
- Lefèvre, M., Lebonnois, S., & Spiga, A. (2018). Three-Dimensional turbulence-resolving modeling of the Venusian cloud layer and induced gravity waves: Inclusion of complete radiative transfer and wind shear. *Journal of Geophysical Research (Planets)*, 123(10), 2773–2789. <https://doi.org/10.1029/2018JE005679>
- Lefèvre, M., Marcq, E., & Lefèvre, F. (2022). The impact of turbulent vertical mixing in the Venus clouds on chemical tracers. *Icarus*, 386, 115148. <https://doi.org/10.1016/j.icarus.2022.115148>
- Lefèvre, M., Spiga, A., & Lebonnois, S. (2017). Three-dimensional turbulence-resolving modeling of the Venusian cloud layer and induced gravity waves. *Journal of Geophysical Research (Planets)*, 122(1), 134–149. <https://doi.org/10.1002/2016JE005146>
- Lefèvre, M., Turbet, M., & Pierrehumbert, R. (2021). 3D convection-resolving model of temperate, tidally locked exoplanets. *The Astrophysical Journal*, 913(2), 101. <https://doi.org/10.3847/1538-4357/abf2c1>
- Määttäinen, A., Guilbon, S., Burgalat, J., & Montmessin, F. (2023). Development of a new cloud model for Venus (MAD-VenLA) using the Modal Aerosol Dynamics approach. *Advances in Space Research*, 71(1), 1116–1136. <https://doi.org/10.1016/j.asr.2022.09.063>
- Marcq, E., Bertaux, J.-L., Montmessin, F., & Belyaev, D. (2013). Variations of Sulphur dioxide at the cloud top of Venus's dynamic atmosphere. *Nature Geoscience*, 6(1), 25–28. <https://doi.org/10.1038/ngeo1650>
- Marcq, E., Bézard, B., Reess, J. M., Henry, F., Éraud, S., Robert, S., et al. (2023). Minor species in Venus' night side troposphere as observed by VIRTIS-H/Venus Express. *Icarus*, 405, 115714. <https://doi.org/10.1016/j.icarus.2023.115714>
- Marcq, E., Lea Jessup, K., Baggio, L., Encrenaz, T., Lee, Y. J., Montmessin, F., et al. (2020). Climatology of SO₂ and UV absorber at Venus' cloud top from SPICAV-UV nadir dataset. *Icarus*, 335, 113368. <https://doi.org/10.1016/j.icarus.2019.07.002>
- Marcq, E., Montmessin, F., Lasue, J., Bézard, B., Jessup, K. L., Lee, Y. J., et al. (2021). Instrumental requirements for the study of Venus' cloud top using the UV imaging spectrometer VeSUV. *Advances in Space Research*, 68(1), 275–291. <https://doi.org/10.1016/j.asr.2021.03.012>
- Markiewicz, W. J., Titov, D. V., Limaye, S. S., Keller, H. U., Ignatiev, N., Jaumann, R., et al. (2007). Morphology and dynamics of the upper cloud layer of Venus. *Nature*, 450(7170), 633–636. <https://doi.org/10.1038/nature06320>
- Marov, M. I., Lystsev, V. E., Lebedev, V. N., Lukashevich, N. L., & Shari, V. P. (1980). The structure and microphysical properties of the Venus clouds: Venera 9, 10, and 11 data. *Icarus*, 44(3), 608–639. [https://doi.org/10.1016/0019-1035\(80\)90131-1](https://doi.org/10.1016/0019-1035(80)90131-1)
- McGouldrick, K., Baines, K. H., Momary, T. W., & Grinspoon, D. H. (2008). Venus Express/VIRTIS observations of middle and lower cloud variability and implications for dynamics. *Journal of Geophysical Research (Planets)*, 113(E5), E00B14. <https://doi.org/10.1029/2008JE003113>
- McGouldrick, K., Momary, T. W., Baines, K. H., & Grinspoon, D. H. (2012). Quantification of middle and lower cloud variability and mesoscale dynamics from Venus Express/VIRTIS observations at 1.74 μm. *Icarus*, 217(2), 615–628. <https://doi.org/10.1016/j.icarus.2011.07.009>
- McGouldrick, K., & Toon, O. B. (2008). Observable effects of convection and gravity waves on the Venus condensational cloud. *Planetary and Space Science*, 56(8), 1112–1131. <https://doi.org/10.1016/j.pss.2008.02.010>
- Oschlisniok, J., Häusler, B., Pätzold, M., Tellmann, S., Bird, M. K., Peter, K., & Andert, T. P. (2021). Sulfuric acid vapor and sulfur dioxide in the atmosphere of Venus as observed by the Venus Express radio science experiment VeRa. *Icarus*, 362, 114405. <https://doi.org/10.1016/j.icarus.2021.114405>
- Peralta, J., Hueso, R., Sánchez-Lavega, A., Piccioni, G., Lanciano, O., & Drossart, P. (2008). Characterization of mesoscale gravity waves in the upper and lower clouds of Venus from VEX-VIRTIS images. *J. of Geophys. Res. (Planets)*, 113(E5), E00B18. <https://doi.org/10.1029/2008JE003185>

- Piccilli, A., Titov, D. V., Sánchez-Lavega, A., Peralta, J., Shalygina, O., Markiewicz, W. J., & Svedhem, H. (2014). High latitude gravity waves at the Venus cloud tops as observed by the Venus monitoring camera on board Venus express. *Icarus*, 227, 94–111. <https://doi.org/10.1016/j.icarus.2013.09.012>
- Rimmer, P. B., Jordan, S., Constantinou, T., Woitke, P., Shorttle, O., Hobbs, R., & Paschodimas, A. (2021). Hydroxide salts in the clouds of Venus: Their effect on the sulfur cycle and cloud droplet pH. *The Planetary Science Journal*, 2(4), 133. <https://doi.org/10.3847/PSJ/ac0156>
- Robert, S., Carine Vandaele, A., Neefs, E., Jacobs, L., Berkenbosch, S., Thomas, I. R., et al. (2019). VenSpec-H, infrared spectrometer onboard EnVision to study Venus' volcanism. In *Epsc-dps joint meeting* (Vol. 13). EPSC-DPS2019.
- Rosow, W. B., del Genio, A. D., Limaye, S. S., Travis, L. D., & Stone, P. H. (1980). Cloud morphology and motions from Pioneer Venus images. *Journal of Geophysical Research*, 85(A13), 8107–8128. <https://doi.org/10.1029/JA085iA13p08107>
- Sagdeev, R. Z., Linkin, V. M., Kerzhanovich, V. V., Lipatov, A. N., Shurupov, A. A., Blamont, J. E., et al. (1986). Overview of VEGA Venus balloon in situ meteorological measurements. *Science*, 231(4744), 1411–1414. <https://doi.org/10.1126/science.231.4744.1411>
- Sato, T. M., Satoh, T., Sagawa, H., Manago, N., Lee, Y. J., Murakami, S., et al. (2020). Dayside cloud top structure of Venus retrieved from Akatsuki IR2 observations. *Icarus*, 345, 113682. <https://doi.org/10.1016/j.icarus.2020.113682>
- Seiff, A., Kirk, D. B., Young, R. E., Blanchard, R. C., Findlay, J. T., Kelly, G. M., & Sommer, S. C. (1980). Measurements of thermal structure and thermal contrasts in the atmosphere of Venus and related dynamical observations - results from the four Pioneer Venus probes. *Journal of Geophysical Research*, 85(A13), 7903–7933. <https://doi.org/10.1029/JA085iA13p07903>
- Skamarock, W. C., & Klemp, J. B. (2008). A time-split nonhydrostatic atmospheric model for weather research and forecasting applications. *Journal of Computational Physics*, 227(7), 3465–3485. <https://doi.org/10.1016/j.jcp.2007.01.037>
- Stolzenbach, A. (2016). *Étude de la photochimie de vénus à l'aide d'un modèle de circulation générale (Doctoral dissertation)*. Thèse de doctorat dirigée par Lefèvre, Franck Sciences Planétaires Paris 6 2016. Retrieved from <http://www.theses.fr/2016PA066413>
- Stolzenbach, A., Lefèvre, F., Lebonnois, S., & Määttä, A. (2023). Three-dimensional modeling of Venus photochemistry and clouds. *Icarus*, 395, 115447. <https://doi.org/10.1016/j.icarus.2023.115447>
- Streel, N., Lefèvre, F., Stolzenbach, A., Määttä, A., Lebonnois, S., Gérard, J. C., & Soret, L. (2023). 3D modelling of the Venus nitrogen chemistry. In *Venus surface and atmosphere*. Held January 30–February 1, 2023 in Houston, Texas and virtually, 2807, 8021.
- Surkov, Y. A., Shcheglov, O. P., Ryvkin, M. L., Sheynin, D. M., Sheynin, D. M., & Davydov, N. A. (1986). The water vapor content profile in the Venusian atmosphere according to the results of experiments from Vega 1 and 2. *Journal of Geophysical Research*, 91(B13), E219–E221. <https://doi.org/10.1029/JB091iB13p0E219>
- Tellmann, S., Haeusler, B., Paetzold, M., Bird, M. K., Tyler, G. L., Andert, T., & Remus, S. (2009). The structure of the Venus neutral atmosphere as seen by the radio science experiment VeRa on Venus express. *J. of Geophys. Res. (Planets)*, 114(E9), E00B36. <https://doi.org/10.1029/2008JE003204>
- Titov, D. V., Markiewicz, W. J., Ignatiev, N. I., Song, L., Limaye, S. S., Sánchez-Lavega, A., et al. (2012). Morphology of the cloud tops as observed by the Venus express monitoring Camera. *Icarus*, 217(2), 682–701. <https://doi.org/10.1016/j.icarus.2011.06.020>
- Vandaele, A. C., Korabev, O., Belyaev, D., Chamberlain, S., Evdokimova, D., Encrenaz, T., et al. (2017). Sulfur dioxide in the Venus atmosphere: II. Spatial and temporal variability. *Icarus*, 295, 1–15. <https://doi.org/10.1016/j.icarus.2017.05.001>
- Woo, R., Armstrong, J. W., & Kliore, A. J. (1982). Small-scale turbulence in the atmosphere of Venus. *Icarus*, 52(2), 335–345. [https://doi.org/10.1016/0019-1035\(82\)90116-6](https://doi.org/10.1016/0019-1035(82)90116-6)
- Woo, R., & Ishimaru, A. (1981). Eddy diffusion coefficient for the atmosphere of Venus from radio scintillation measurements. *Nature*, 289(5796), 383–384. <https://doi.org/10.1038/289383a0>
- Yung, Y. L., Liang, M. C., Jiang, X., Shia, R. L., Lee, C., Bézard, B., & Marq, E. (2009). Evidence for carbonyl sulfide (OCS) conversion to CO in the lower atmosphere of Venus. *Journal of Geophysical Research (Planets)*, 114(16), E00B34. <https://doi.org/10.1029/2008JE003094>